



Published in final edited form as:

*Hum Genet.* 2018 March ; 137(3): 195–202. doi:10.1007/s00439-017-1864-x.

## Genetic and functional analysis of *SHROOM1-4* in a Chinese neural tube defect cohort

Zhongzhong Chen<sup>1,2</sup>, Lele Kuang<sup>1,2</sup>, Richard H. Finnell<sup>1,2,3,4</sup>, and Hongyan Wang<sup>1,2,5</sup>

<sup>1</sup>Obstetrics and Gynecology Hospital, State Key Laboratory of Genetic Engineering at School of Life Sciences, Institute of Reproduction and Development, Fudan University, Shanghai 200011, China

<sup>2</sup>Key Laboratory of Reproduction Regulation of NPFPC, Collaborative Innovation Center of Genetics and Development, Fudan University, Shanghai 200032, China

<sup>3</sup>Departments of Molecular and Cellular Biology and Medicine, Baylor College of Medicine, Houston, TX 77030, USA

<sup>4</sup>Collaborative Innovation Center for Genetics and Development, School of Life Sciences, Fudan University, Jiangwan Campus, Shanghai 200438, China

<sup>5</sup>Children's Hospital and Institutes of Biomedical Sciences of Fudan University, Shanghai, China

### Abstract

Neural tube defects (NTDs), which include spina bifida and anencephaly, are the second most common form of human structural congenital malformations. While it is well established that *SHROOM3* plays a pivotal role in the complex morphogenetic processes involved in neural tube closure (NTC), the underlying genetic contributions of *SHROOM* gene family members in the etiology of human NTDs remain poorly understood. Herein, we systematically investigated the mutation patterns of *SHROOM1-4* in a Chinese population composed of 343 NTD cases and 206 controls, using targeted next-generation sequencing. Functional variants were further confirmed by western blot and the mammalian two-hybrid assays. Loss of function (LoF) variants were identified in *SHROOM3*. We observed 1.56 times as many rare [minor allele frequency (MAF) < 0.01] coding variants ( $p = 2.9 \times 10^{-3}$ ) in *SHROOM* genes, and 4.5 times as many rare D-Mis (deleterious missense) variants in *SHROOM2* genes in the NTD cases compared with the controls. D-Mis variants of *SHROOM2* (p.A1331S; p.R1557H) were confirmed by Sanger sequencing, and these variants were determined to have profound effects on gene function that disrupted their binding with ROCK1 in vitro. These findings provide genetic and molecular insights into the effects of rare damaging variants in *SHROOM2*, indicating that such variants of *SHROOM2* might

---

Zhongzhong Chen and Lele Kuang contributed equally.

Electronic supplementary material The online version of this article (<https://doi.org/10.1007/s00439-017-1864-x>) contains supplementary material, which is available to authorized users.

**Author contributions** HW and ZC directed and designed the study. ZC performed statistical and bioinformatics analysis. LK performed functional validation. HW, ZC, RF, and LK prepared the manuscript; all authors reviewed the manuscript.

**Compliance with ethical standards**

**Conflict of interest** The author declares no competing financial interests.

contribute to the risk of human NTDs. This research enhances our understanding of the genetic contribution of the *SHROOM* gene family to the etiology of human NTDs.

---

## Introduction

Failure of neural tube closure (NTC) leads to severe birth defects, such as anencephaly and spina bifida, more commonly known as neural tube defects (NTDs). The prevalence statistics indicate that NTDs occur in 5 per 10,000 live births in the United States (Wallingford et al. 2013) and at a considerably higher rate in China (138.7/10,000) (Li et al. 2006). In higher vertebrates, the neural tube proceeds initially with the formation of the neural plate, followed by the elevation, bending and fusion of the neural folds to become a closed tube. These complicated processes are regulated by multiple mechanisms, including coordination of the activity of Rho kinase (ROCK) and the planar cell polarity (PCP) pathways. More than 400 different mouse genes with diverse cellular functions have been implicated as genetic risk factors for NTDs (Harris and Juriloff 2010). At the present time, none of the mouse NTD candidate genes adequately informs our understanding of the genetic basis underlying the etiology of human NTDs.

Two morphogenetic processes, neural plate apical constriction and convergent extension, are required for neural tube closure (Nishimura et al. 2012). PCP molecules have been recognized as linking these two morphogenetic processes in the neural tube (Copp and Greene 2010; Nishimura et al. 2012). Genetic modification of PCP core genes in mouse models, such as *Vangl2* and *Celsr1*, lead to severe NTDs, indicating that there is a strong connection between PCP signaling and risk for NTDs (Murdoch et al. 2014). PCP-dependent convergent extension is crucial for NTC, and loss of function (LoF) alleles of *Vangl2* (Greene et al. 1998), *Celsr1* (Curtin et al. 2003), *Frizzled3* (*Fz3*) (Wang et al. 2006), *Frizzled6* (*Fz6*) (Wang et al. 2006), *Dvl1* and *Dvl2* (Etheridge et al. 2008) cause craniorachischisis. Recently, *SHROOM3* was demonstrated to function downstream of the PCP pathway to regulate myosin II distribution and cellular behavior to promote NTC in mouse models (McGreevy et al. 2015). *SHROOM3* is a cytoskeleton regulating protein that contains three evolutionarily conserved domains. The ASD1 and ASD2 domains lie in the N- and C-terminal, while the PDZ domain is located in the central region. Previous studies showed that neuroepithelial cells in homozygous *SHROOM* knockout mouse embryos failed to converge in the dorsal midline resulting in exencephaly and spina bifida phenotypes (Hildebrand and Soriano 1999). In *Xenopus* embryos, *SHROOM* induces apical constriction to regulate the formation of hinge points during NTC (Haigo et al. 2003). In zebrafish embryos, knock down of *SHROOM3* blocks apical constriction (Ernst et al. 2012). In polarized epithelia, induced expression of *SHROOM* elicits apical constriction and reorganization of the actomyosin network (Hildebrand 2005). Rho/ROCK signaling promotes actomyosin contractility (Rath and Olson 2012), which is utilized for controlling cell shape and behavior. Exposure to inhibitors of Myosin II or ROCK resulted in NTDs due to failed apical constriction and convergent extension (Kinoshita et al. 2008). *SHROOM3* can directly interact with Rho kinase (ROCK) through the ASD2 domain (Nishimura and Takeichi 2008), which is highly conserved in the *SHROOM* gene family (Hildebrand and

Soriano 1999). Finally, the interaction between *SHROOM3* and *ROCK* plays a pivotal role during neural tube morphogenesis (Das et al. 2014).

Animal models and human NTD cohort studies have made it clear that *SHROOM3* is involved in NTD etiology (Haigo et al. 2003; Hildebrand and Soriano 1999; Lemay et al. 2015). The importance of *SHROOM3* in NTC is beyond dispute, and a recent study identified two protein truncating de novo mutations in *SHROOM3* in human NTD patients (Lemay et al. 2015). However, the genetic contributions of other *SHROOM* family members in NTDs have remained elusive. The excess of damaging variants, including LoF (loss of function, including splice acceptor/donor, stop gained/lost, initiator codon and frameshift indels) and D-mis (deleterious missense) variants, were used in identifying causal genes in birth defect diseases, such as congenital heart disease (Homsy et al. 2015) and craniosynostosis (Timberlake et al. 2016). To better understand human NTD risk-associated damaging variants of *SHROOM* family genes and their underlying biological mechanisms, we systematically investigated the mutation patterns of *SHROOM1-4* in a Chinese population composed of 343 NTD and 206 control-genomic DNA samples.

## Materials and methods

### The Chinese NTD study population

We implemented a two-stage design for this study. Subjects in the capture sequencing stage, consisting of 343 aborted fetuses with NTDs and 206 blood samples from healthy controls, were all ethnically Han Chinese, as previously described (Lei et al. 2010; Shi et al. 2012; Yang et al. 2013). This study was approved by the Ethics Committee of the School of Life Sciences, Fudan University. All of these samples were received with informed parental consent.

### DNA sequencing, genotyping and data analysis

The genomic structure of human *SHROOM1-4* genes were determined using NCBI GenBank (NM\_133456, NM\_001649, NM\_020859 and NM\_020717). The 5'-UTR, 3'-UTR, and coding regions in *SHROOM1-4* were detected by targeted next-generation sequencing. Sequencing was performed on Illumina GAI (Illumina, San Diego, CA, USA) platform using the paired-end program. Variant calling and annotation was performed using previously established methods (Qiao et al. 2016). Coding variants were classified as synonymous, missense, LoF (loss of function, including splice acceptor/donor, stop gained/lost, initiator codon and frameshift indels) and others using Variant Effect Predictor (VEP) (McLaren et al. 2010). PolyPhen-2 (Adzhubei et al. 2010) and SIFT (Kumar et al. 2009; Sim et al. 2012) were utilized to predict the genomic consequences of missense mutations via VEP tools. The missense variants that were predicted to be damaging by PolyPhen-2 or deleterious by SIFT were annotated as deleterious missense variants (D-mis). Two variants, identified by targeted capture sequencing and considered likely to be damaging, were selected to be further validated by Sanger sequencing.

Binomial testing as previously used in congenital heart disease study (Homsy et al. 2015), was performed for burden analysis of rare coding variants by comparisons of NTD cases and controls. Statistical analyses were performed by R (<http://www.R-project.org>).

### Plasmid construction

Myc-DDK tagged human *SHROOM2* (NM\_001649) cDNA was purchased from OriGene Technologies (Beijing, China). Human *ROCK1* (NM\_005406) was purchased from YouBio (Hunan, China). The ASD2 domain (aa1317-1611) was PCR amplified from *SHROOM2* cDNA and inserted into the pCMV6-Entry empty vector at the SgfI-MluI restriction sites. All mutations in *SHROOM2* were generated using a QuickChange Site-Directed Mutagenesis Kit (Stratagene). The SHROOM binding domain (SBD) of *ROCK1* was inserted into pCMV6-HA empty vector at the SgfI-MluI restriction sites. For the CheckMate™ Mammalian Two-Hybrid system, the bait constructs were PCR amplified from *SHROOM2* and *ROCK1* cDNAs. The ASD2 domains (aa1317-1611) of *SHROOM2* wildtype and mutant sequences were subcloned into pBIND vectors and fused in-frame with GAL4 at SalI and XbaI restriction sites. The SBD located in *ROCK1* was cloned into the pACT vector and fused with VP16 in-frame at the same restriction sites as the pBIND vector.

All plasmids used in this study were confirmed by DNA sequencing, and the primers used for plasmid construction are listed in Table S1.

### Western blot and Co-immunoprecipitation

Myc-DDK tagged *SHROOM2-ASD2* wildtype or mutant was co-transfected into HEK293T cells with pCMV6-GFP empty vector. Twenty-four hours later, cells were harvested with lysis buffer [50 mM of Tris (pH7.4), 150 mM of NaCl, 1% NP-40, 0.25% sodium deoxycholate, protease inhibitors]. Samples were loaded and separated on a 10% SDS-PAGE gel and were then transferred to a polyvinylidenedifluoride (PVDF) membrane (Millipore). After blocking for 1 h with 5% non-fat milk, the membrane was incubated with the primary antibody at 4 °C overnight. ECL was used to visualize the protein bands after incubating with secondary antibody for 1 h at room temperature. GFP empty vector was used as a transfection efficiency control.

A co-immunoprecipitation assay was further performed to evaluate whether there is an interaction between *SHROOM2* and *ROCK1*. Myc-DDK tagged *SHROOM2-ASD2* wildtype or mutant was co-transfected into HEK293T cells with HA-tagged *ROCK1-SBD*. Lysates were produced in lysis buffer and incubated with anti-Myc agarose beads (Abmart) at 4 °C for 2 h. After washing five times with lysis buffer, the beads were collected by centrifugation, eluted in 1× SDS loading buffer, boiled at 100 °C for 10 min, and analyzed by western blotting. Band density of target proteins was quantitatively analyzed using Image J. The band density ratios of IB:HA (upper) relative to IP:Myc were used to measure the binding ability to *ROCK1* between wildtype and mutants. Four independent experiments were performed and representative results were shown.

## CheckMate™ Mammalian Two-Hybrid system

The CheckMate™ Mammalian Two-Hybrid System (Promega), which contains three plasmids, was used for detecting protein–protein interactions. The pGL4.3luc vector is a firefly luciferase reporter plasmid containing five GAL4 binding sites. The pACT vector has a VP16 domain that can activate the firefly luciferase expression when it binds to GAL4. The pBIND vector, which has a GAL4 DNA-binding domain, is used to express Renilla luciferase and normalize the transfection efficiency. When two proteins of interest are fused with GAL4 and VP16 separately, firefly luciferase activity will increase compared to the negative control, if such a positive interaction exists. To test the interaction between SHROOM2 and ROCK1, HEK293T cells were co-transfected with the above-indicated plasmids using Lipofectamine 2000 (Invitrogen). Twenty-four hours post-transfection, cells were harvested for a luciferase assay, and the ratios of firefly and Renilla luciferase activities were determined.

## Results

### Enrichment of rare coding variants in *SHROOM* genes

In this study, we sequenced the coding regions of *SHROOM1-4* from 343 NTD and 206 normal control samples by targeted next-generation sequencing, and detected 161 and 62 rare coding variants in the NTD samples and controls, respectively ( $MAF < 0.01$ ). To interrogate the rare coding variants of *SHROOM* family genes, a burden test was performed based on a binomial test. The results indicated that rare coding variants were markedly increased in NTDs compared with controls (enrichment = 1.56,  $p = 2.9 \times 10^{-3}$ ) (Table 1). We also observed significant enrichment of rare missense variants of 1.65 ( $p = 6.8 \times 10^{-3}$ ) in *SHROOM1-4*. To evaluate the genomic effects of the mutations, we grouped coding variants into synonymous, missense, D-mis, LoF, damaging (LoF and D-mis) and other mutation types. One LoF variant, frameshift variant p.N594fs in *SHROOM3*, was identified in NTD cases, but LoF variants were not significantly enriched in the NTD cohort. We subsequently analyzed the total burden of rare damaging variants in *SHROOM1-4*. No significant enrichments of D-Mis variants were found in *SHROOM1*, *SHROOM3* and *SHROOM4*. However, we detected significant 4.5-fold enrichment of D-Mis variants in *SHROOM2* ( $p = 0.04$ ).

### Rare damaging variants of *SHROOM2* with diverse NTD phenotypes

Among all 42 detected *SHROOM2* variants in the 343 NTD samples, 15 rare damaging mutants were identified from 15 NTD samples (Table 2). The 15 mutants were distributed among eight loci (Fig. 1). All of these damaging mutants are very rare in the ExAC database, with  $MAF < 0.001$ , and four of the variants were novel and did not exist in ExAC (Table 2). Samples with rare damaging variants were observed to have different NTD phenotypes (Table 2). Sample D56 with p.S1219R, and samples D42 and D44 with p.R1557H were from fetuses with anencephaly. Sample D20 with p.A119T, T9 with p.G1349V and D117 with p.R1557H were spina bifida cases. Sample SY3180 and SZNT6 with p.A1331S, D125 with p.A1470T and D135 with p.R1557H displayed encephalocele phenotypes. Five other patients were observed to have mixed or multiple NTD phenotypes.

### Damaging variants of *SHROOM2* significantly decreased interactions with ROCK1

*SHROOM* proteins interact with ROCK1 through its conserved ASD2 domain to direct its subcellular localization and participate in regulating cytoskeletal dynamics (Zalewski et al. 2016). The two damaging variants (p.A1331S and p.R1557H) with the highest frequencies (4/15 and 5/15, respectively) were located in the ASD2 domain (Fig. 1). These two variants were confirmed by Sanger sequencing (Fig. 2a, b). We further evaluated whether these D-Mis variants of *SHROOM2* were functional variants using western blot and the CheckMate™ Mammalian Two-Hybrid system. These two investigated *SHROOM2* D-Mis variants (p.A1331S and p.R1557H) have no significant effects on protein expression (Fig. 2c). However, the interactions of these two *SHROOM2* D-Mis variants with ROCK1 were significantly decreased using the CheckMate™ Mammalian Two-Hybrid system (Fig. 2d). Additionally, the interaction between *SHROOM2* ASD2 domain and ROCK1 SBD was validated by co-immunoprecipitation (Fig. 2e), and both *SHROOM2* mutations significantly decreased their interaction with ROCK1 SBD (Fig. 2f). This suggests that deleterious variants of *SHROOM2* attenuate their interaction with ROCK1 which can have significant consequences during NTC.

### Discussion

*SHROOM3* mediates the PCP pathway (McGreevy et al. 2015) and plays an essential role in regulating cytoskeletal dynamics (Zalewski et al. 2016), which are critically important during the closure of the neural tube. Recently, de novo LoF mutations in *SHROOM3* were experimentally associated with the development of NTDs, suggesting that these variants may also contribute to the genetic etiology of severe human NTDs (Lemay et al. 2015). However, the genetic contributions of other *SHROOM* family members to human NTDs have not been previously reported. In this study, we systematically investigated the mutation patterns of *SHROOM1-4* in a Han Chinese NTD cohort. Our results suggest that rare coding variants in the *SHROOM* gene family were markedly increased in NTD patients, and that rare damaging variants of *SHROOM2* might also contribute to the risk for human NTDs by adversely affecting interactions of *SHROOM2*-ROCK1, which are involved in both the PCP pathway and cytoskeletal regulation.

PCP molecules control the morphogenetic processes of apical constriction and convergent extension, which are required for NTC (Copp and Greene 2010; Nishimura et al. 2012). The association between rare mutations of PCP-related genes and human NTDs has been well studied (Allache et al. 2012; Bosoi et al. 2011; De Marco et al. 2012; Kibar et al. 2007; Robinson et al. 2012; Seo et al. 2015). Previous animal models have demonstrated that homozygous *Shroom3* mutant embryos exhibited exencephaly (Hildebrand and Soriano 1999). *Shroom3* interacts genetically with the PCP components *Vangl2* and *Wnt5a*, and depletion of *Shroom3* and *Vangl2* or *Wnt5a* can drastically increase the penetrance and severity of NTDs (McGreevy et al. 2015). The PCP pathway is highly dosage sensitive, and over- or under-expression of PCP core genes in zebrafish and *Xenopus* embryos results in convergent extension defects (Roszko et al. 2009; Wallingford 2005, 2013). Our results identified a LoF variant p.N594fs in *SHROOM3*. Despite the dysregulation of the PCP

pathway induced by rare LoF mutants of *SHROOM3* might contribute the risk of human NTDs; there is no significant enrichment of D-Mis variants in *SHROOM3*.

*SHROOM2* is significantly enriched in D-Mis variants in our study, suggesting that it is likely to be pathogenic for NTDs. ROCK1 is a serine/threonine kinase whose activity drives cytoskeletal regulation associated with apical constriction (Das et al. 2014; Haigo et al. 2003; Hildebrand 2005). *SHROOM3* can regulate NTC through interactions with the SBD domain of ROCK1 in vertebrates (Das et al. 2014; Hildebrand 2005), indicating that *SHROOM2* may have similar molecular activities. Moreover, we verified that these two damaging variants (p.A1331S and p.R1557H) in *SHROOM2* significantly decreased the interaction between *SHROOM2* and ROCK1 (Fig. 2). Collectively, our study provided strong direct evidence that rare damaging mutations in *SHROOM2* impaired *SHROOM2*-ROCK1 binding, which would suggest that rare damaging variants in *SHROOM2* result in the misregulation of ROCK1, leading to an alteration of cytoskeletal remodeling.

Despite the importance of demonstrating *SHROOM*-mediated remodeling in the etiology of NTDs using a mouse model, the genetic contributions and the underlying molecular mechanisms of *SHROOM* gene family members in human NTD patients were lacking. We systematically investigated the mutation patterns of *SHROOM1-4* via case-control burden analysis in a Han Chinese population, and further performed in vitro functional confirmation studies. The results suggested that damaging variants in *SHROOM2* are likely to play major roles in contributing to NTD risk. We provided molecular insight into the effects of rare damaging variants in *SHROOM2*-ROCK1 binding, indicating that rare damaging variants of *SHROOM2* might lead to the misregulation of PCP signaling and alterations in cytoskeletal remodeling that contribute to the risk of human NTDs.

## Supplementary Material

Refer to Web version on PubMed Central for supplementary material.

## Acknowledgments

This work was supported by Grants from the 973 Program (2013CB945403), the National Natural Science Foundation of China (81430005, 31521003), National key research and development program (2016YFC1000502), and the Commission for Science and Technology of Shanghai Municipality (17JC1400902) to H. Wang. Dr. Finnell was supported by NIH grant P01 HD067244.

## References

- Adzhubei IA, Schmidt S, Peshkin L, Ramensky VE, Gerasimova A, Bork P, Kondrashov AS, Sunyaev SR. A method and server for predicting damaging missense mutations. *Nat Methods*. 2010; 7:248–249. <https://doi.org/10.1038/nmeth0410-248>. [PubMed: 20354512]
- Allache R, De Marco P, Merello E, Capra V, Kibar Z. Role of the planar cell polarity gene CELSR1 in neural tube defects and caudal agenesis. *Birth Defects Res A Clin Mol Teratol*. 2012; 94:176–181. <https://doi.org/10.1002/bdra.23002>. [PubMed: 22371354]
- Bosoi CM, Capra V, Allache R, Trinh VQ, De Marco P, Merello E, Drapeau P, Bassuk AG, Kibar Z. Identification and characterization of novel rare mutations in the planar cell polarity gene PRICKLE1 in human neural tube defects. *Hum Mutat*. 2011; 32:1371–1375. <https://doi.org/10.1002/humu.21589>. [PubMed: 21901791]

- Copp AJ, Greene ND. Genetics and development of neural tube defects. *J Pathol.* 2010; 220:217–230. <https://doi.org/10.1002/path.2643>. [PubMed: 19918803]
- Curtin JA, Quint E, Tspouri V, Arkell RM, Cattanaach B, Copp AJ, Henderson DJ, Spurr N, Stanier P, Fisher EM, Nolan PM, Steel KP, Brown SD, Gray IC, Murdoch JN. Mutation of *Celsr1* disrupts planar polarity of inner ear hair cells and causes severe neural tube defects in the mouse. *Curr Biol.* 2003; 13:1129–1133. [PubMed: 12842012]
- Das D, Zalewski JK, Mohan S, Plageman TF, VanDemark AP, Hildebrand JD. The interaction between Shroom3 and Rhokinase is required for neural tube morphogenesis in mice. *Biol Open.* 2014; 3:850–860. <https://doi.org/10.1242/bio.20147450>. [PubMed: 25171888]
- De Marco P, Merello E, Rossi A, Piatelli G, Cama A, Kibar Z, Capra V. FZD6 is a novel gene for human neural tube defects. *Hum Mutat.* 2012; 33:384–390. <https://doi.org/10.1002/humu.21643>. [PubMed: 22045688]
- Ernst S, Liu K, Agarwala S, Moratscheck N, Avci ME, Dalle Nogare D, Chitnis AB, Ronneberger O, Lecaudey V. Shroom3 is required downstream of FGF signalling to mediate proneuromast assembly in zebrafish. *Development.* 2012; 139:4571–4581. <https://doi.org/10.1242/dev.083253>. [PubMed: 23136387]
- Etheridge SL, Ray S, Li S, Hamblet NS, Lijam N, Tsang M, Greer J, Kardos N, Wang J, Sussman DJ, Chen P, Wynshaw-Boris A. Murine dishevelled 3 functions in redundant pathways with dishevelled 1 and 2 in normal cardiac outflow tract, cochlea, and neural tube development. *PLoS Genet.* 2008; 4:e1000259. <https://doi.org/10.1371/journal.pgen.1000259>. [PubMed: 19008950]
- Greene ND, Gerrelli D, Van Straaten HW, Copp AJ. Abnormalities of floor plate, notochord and somite differentiation in the loop-tail (Lp) mouse: a model of severe neural tube defects. *Mech Dev.* 1998; 73:59–72. [PubMed: 9545534]
- Haigo SL, Hildebrand JD, Harland RM, Wallingford JB. Shroom induces apical constriction and is required for hinge-point formation during neural tube closure. *Curr Biol.* 2003; 13:2125–2137. [PubMed: 14680628]
- Harris MJ, Juriloff DM. An update to the list of mouse mutants with neural tube closure defects and advances toward a complete genetic perspective of neural tube closure. *Birth Defects Res A Clin Mol Teratol.* 2010; 88:653–669. <https://doi.org/10.1002/bdra.20676>. [PubMed: 20740593]
- Hildebrand JD. Shroom regulates epithelial cell shape via the apical positioning of an actomyosin network. *J Cell Sci.* 2005; 118:5191–5203. <https://doi.org/10.1242/jcs.02626>. [PubMed: 16249236]
- Hildebrand JD, Soriano P. Shroom, a PDZ domain-containing actin-binding protein, is required for neural tube morphogenesis in mice. *Cell.* 1999; 99:485–497. [PubMed: 10589677]
- Homsy J, Zaidi S, Shen Y, Ware JS, Samocha KE, Karczewski KJ, DePalma SR, McKean D, Wakimoto H, Gorham J, Jin SC, Deanfield J, Giardini A, Porter GA Jr, Kim R, Bilguvar K, Lopez-Giraldez F, Tikhonova I, Mane S, Romano-Adesman A, Qi H, Vardarajan B, Ma L, Daly M, Roberts AE, Russell MW, Mital S, Newburger JW, Gaynor JW, Breitbart RE, Iossifov I, Ronemus M, Sanders SJ, Kaltman JR, Seidman JG, Brueckner M, Gelb BD, Goldmuntz E, Lifton RP, Seidman CE, Chung WK. De novo mutations in congenital heart disease with neurodevelopmental and other congenital anomalies. *Science.* 2015; 350:1262–1266. <https://doi.org/10.1126/science.aac9396>. [PubMed: 26785492]
- Kibar Z, Torban E, McDearmid JR, Reynolds A, Berghout J, Mathieu M, Kirillova I, De Marco P, Merello E, Hayes JM, Wallingford JB, Drapeau P, Capra V, Gros P. Mutations in *VANGL1* associated with neural-tube defects. *N Engl J Med.* 2007; 356:1432–1437. <https://doi.org/10.1056/NEJMoa060651>. [PubMed: 17409324]
- Kinoshita N, Sasai N, Misaki K, Yonemura S. Apical accumulation of Rho in the neural plate is important for neural plate cell shape change and neural tube formation. *Mol Biol Cell.* 2008; 19:2289–2299. <https://doi.org/10.1091/mbc.E07-12-1286>. [PubMed: 18337466]
- Kumar P, Henikoff S, Ng PC. Predicting the effects of coding non-synonymous variants on protein function using the SIFT algorithm. *Nat Protoc.* 2009; 4:1073–1081. <https://doi.org/10.1038/nprot.2009.86>. [PubMed: 19561590]
- Lei YP, Zhang T, Li H, Wu BL, Jin L, Wang HY. *VANGL2* mutations in human cranial neural-tube defects. *N Engl J Med.* 2010; 362:2232–2235. <https://doi.org/10.1056/NEJMc0910820>. [PubMed: 20558380]



- Lemay P, Guyot MC, Tremblay E, Dionne-Laporte A, Spiegelman D, Henrion E, Diallo O, De Marco P, Merello E, Massicotte C, Desilets V, Michaud JL, Rouleau GA, Capra V, Kibar Z. Loss-of-function de novo mutations play an important role in severe human neural tube defects. *J Med Genet*. 2015; 52:493–497. <https://doi.org/10.1136/jmedgenet-2015-103027>. [PubMed: 25805808]
- Li Z, Ren A, Zhang L, Ye R, Li S, Zheng J, Hong S, Wang T, Li Z. Extremely high prevalence of neural tube defects in a 4-county area in Shanxi Province, China. *Birth Defects Res A Clin Mol Teratol*. 2006; 76:237–240. <https://doi.org/10.1002/bdra.20248>. [PubMed: 16575897]
- McGreevy EM, Vijayraghavan D, Davidson LA, Hildebrand JD. Shroom3 functions downstream of planar cell polarity to regulate myosin II distribution and cellular organization during neural tube closure. *Biol Open*. 2015; 4:186–196. <https://doi.org/10.1242/bio.20149589>. [PubMed: 25596276]
- McLaren W, Pritchard B, Rios D, Chen Y, Flicek P, Cunningham F. Deriving the consequences of genomic variants with the Ensembl API and SNP Effect Predictor. *Bioinformatics*. 2010; 26:2069–2070. <https://doi.org/10.1093/bioinformatics/btq330>. [PubMed: 20562413]
- Murdoch JN, Damrau C, Paudyal A, Bogani D, Wells S, Greene ND, Stanier P, Copp AJ. Genetic interactions between planar cell polarity genes cause diverse neural tube defects in mice. *Dis Model Mech*. 2014; 7:1153–1163. <https://doi.org/10.1242/dmm.016758>. [PubMed: 25128525]
- Nishimura T, Takeichi M. Shroom3-mediated recruitment of Rho kinases to the apical cell junctions regulates epithelial and neuroepithelial planar remodeling. *Development*. 2008; 135:1493–1502. <https://doi.org/10.1242/dev.019646>. [PubMed: 18339671]
- Nishimura T, Honda H, Takeichi M. Planar cell polarity links axes of spatial dynamics in neural-tube closure. *Cell*. 2012; 149:1084–1097. <https://doi.org/10.1016/j.cell.2012.04.021>. [PubMed: 22632972]
- Qiao, X., Liu, Y., Li, P., Chen, Z., Li, H., Yang, X., Finnell, RH., Yang, Z., Zhang, T., Qiao, B., Zheng, Y., Wang, H. Genetic analysis of rare coding mutations in CELSR1-3 in Chinese congenital heart and neural tube defects. *Clin Sci (Lond)*. 2016. <https://doi.org/10.1042/CS20160686>
- Rath N, Olson MF. Rho-associated kinases in tumorigenesis: re-considering ROCK inhibition for cancer therapy. *EMBO Rep*. 2012; 13:900–908. <https://doi.org/10.1038/embor.2012.127>. [PubMed: 22964758]
- Robinson A, Escuin S, Doudney K, Vekemans M, Stevenson RE, Greene ND, Copp AJ, Stanier P. Mutations in the planar cell polarity genes CELSR1 and SCRIB are associated with the severe neural tube defect craniorachischisis. *Hum Mutat*. 2012; 33:440–447. <https://doi.org/10.1002/humu.21662>. [PubMed: 22095531]
- Roszkó I, Sawada A, Solnica-Krezel L. Regulation of convergence and extension movements during vertebrate gastrulation by the Wnt/PCP pathway. *Semin Cell Dev Biol*. 2009; 20:986–997. <https://doi.org/10.1016/j.semcdb.2009.09.004>. [PubMed: 19761865]
- Seo JH, Zilber Y, Babayeva S, Liu J, Kyriakopoulos P, De Marco P, Merello E, Capra V, Gros P, Torban E. Mutations in the planar cell polarity gene, Fuzzy, are associated with neural tube defects in humans. *Hum Mol Genet*. 2015; 24:3893. <https://doi.org/10.1093/hmg/ddv131>. [PubMed: 25954026]
- Shi Y, Ding Y, Lei YP, Yang XY, Xie GM, Wen J, Cai CQ, Li H, Chen Y, Zhang T, Wu BL, Jin L, Chen YG, Wang HY. Identification of novel rare mutations of DACT1 in human neural tube defects. *Hum Mutat*. 2012; 33:1450–1455. <https://doi.org/10.1002/humu.22121>. [PubMed: 22610794]
- Sim NL, Kumar P, Hu J, Henikoff S, Schneider G, Ng PC. SIFT web server: predicting effects of amino acid substitutions on proteins. *Nucleic Acids Res*. 2012; 40:W452–W457. <https://doi.org/10.1093/nar/gks539>. [PubMed: 22689647]
- Timberlake AT, Choi J, Zaidi S, Lu Q, Nelson-Williams C, Brooks ED, Bilguvar K, Tikhonova I, Mane S, Yang JF, Sawh-Martinez R, Persing S, Zellner EG, Loring E, Chuang C, Galm A, Hashim PW, Steinbacher DM, DiLuna ML, Duncan CC, Pelphey KA, Zhao H, Persing JA, Lifton RP. Two locus inheritance of non-syndromic midline craniosynostosis via rare SMAD6 and common BMP2 alleles. *Elife*. 2016; 5:e20125. <https://doi.org/10.7554/eLife.20125>. [PubMed: 27606499]
- Wallingford JB. Neural tube closure and neural tube defects: studies in animal models reveal known knowns and known unknowns. *Am J Med Genet C Semin Med Genet*. 2005; 135C:59–68. <https://doi.org/10.1002/ajmg.c.30054>. [PubMed: 15806594]

- Wallingford JB, Niswander LA, Shaw GM, Finnell RH. The continuing challenge of understanding, preventing, and treating neural tube defects. *Science*. 2013; 339:1222002. <https://doi.org/10.1126/science.1222002>. [PubMed: 23449594]
- Wang Y, Guo N, Nathans J. The role of Frizzled3 and Frizzled6 in neural tube closure and in the planar polarity of inner-ear sensory hair cells. *J Neurosci*. 2006; 26:2147–2156. <https://doi.org/10.1523/JNEUROSCI.4698-05.2005>. [PubMed: 16495441]
- Yang XY, Zhou XY, Wang QQ, Li H, Chen Y, Lei YP, Ma XH, Kong P, Shi Y, Jin L, Zhang T, Wang HY. Mutations in the COPII vesicle component gene SEC24B are associated with human neural tube defects. *Hum Mutat*. 2013; 34:1094–1101. <https://doi.org/10.1002/humu.22338>. [PubMed: 23592378]
- Zalewski JK, Mo JH, Heber S, Heroux A, Gardner RG, Hildebrand JD, VanDemark AP. Structure of the Shroom–Rho kinase complex reveals a binding interface with monomeric shroom that regulates cell morphology and stimulates kinase activity. *J Biol Chem*. 2016; 291:25364–25374. <https://doi.org/10.1074/jbc.M116.738559>. [PubMed: 27758857]

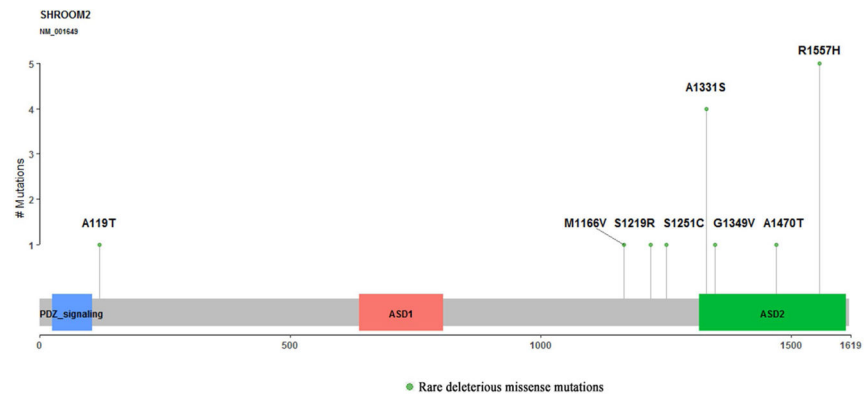


**Fig. 1.**  
Mapping of rare damaging mutations affecting *SHROOM2*

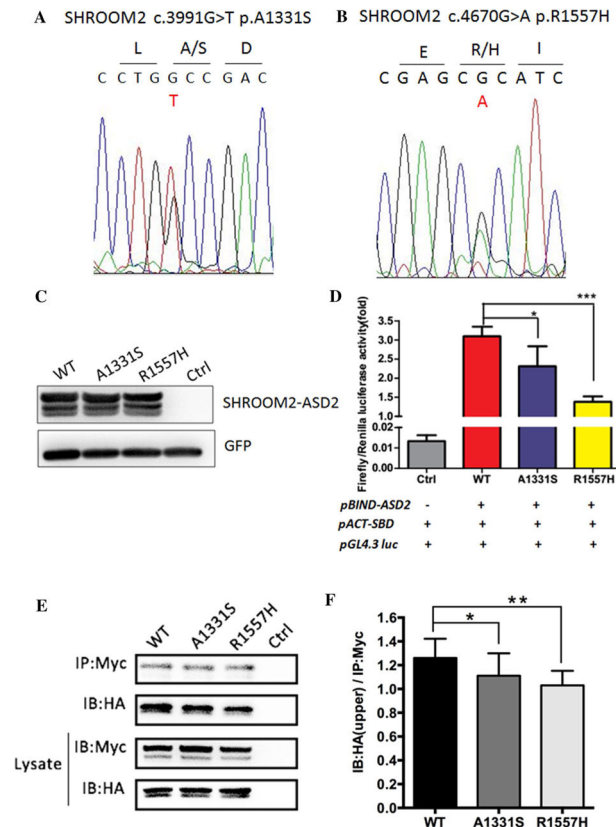


**Fig. 2.** Deleterious variants of SHROOM2 attenuate their interactions with ROCK1. **a, b** Sanger sequencing results showed heterozygous missense mutants *SHROOM2* c.3991G > T (p.A1331S) and *SHROOM2* c.4670G > A (p.R1557H). **c** Western blot analysis of HEK293T cells transfected with *SHROOM2-ASD2* wildtype, mutant or empty vector. GFP was co-transfected and used to normalize transfection efficiency. **d** The interactions of these two *SHROOM2* D-Mis variants with ROCK1 were significantly decreased using the CheckMate™ Mammalian Two-Hybrid system. Various combinations of plasmids were transfected into HEK293T cells as indicated. **e** Co-immunoprecipitation (Co-IP) assay also validated the reduced interaction between SHROOM2 ASD2 domain and ROCK1 SBD. **f** Quantitative analysis of Co-IP results in **e**. Band density ratios were calculated and analyzed between wildtype and indicated *SHROOM2* variants. Four independent experiments were performed and the asterisk indicates a statistical difference (\* $p < 0.05$ , \*\* $p < 0.01$ , \*\*\* $p < 0.001$ ) by Student's *t* test

**Table 1**

Burden analysis by comparisons of NTD cases vs. controls

	Cases, <i>N</i> = 343	Controls, <i>N</i> = 206	OR	<i>p</i> <sup><i>b</i></sup>
All genes				
Total <sup><i>a</i></sup>	161	62	1.56	$2.9 \times 10^{-3}$
Synonymous	46	16	1.73	0.066
Missense	110	40	1.65	$6.8 \times 10^{-3}$
D-Mis	41	17	1.49	0.223
LoF	1	0	NA	1
Damaging	42	17	1.48	0.181
D-Mis <i>SHROOM1-4</i>	41	17	1.49	0.223
D-Mis <i>SHROOM1</i>	4	4	0.6	0.484
D-Mis <i>SHROOM2</i>	15	2	4.50	0.041
D-Mis <i>SHROOM3</i>	13	5	1.56	0.472
D-Mis <i>SHROOM4</i>	9	6	0.9	1

<sup>*a*</sup>Total: rare coding variants with MAF < 0.01<sup>*b*</sup>*p* value based on binomial test

Table 2

Rare damaging mutations in *SHROOM2* with diverse NTD phenotypes

Sample	Variant	Chr.	Position <sup>d</sup>	Minor/major allele	Sex	Phenotype	SIFT <sup>b</sup>	PP2 <sup>c</sup>	MAF in ExAC <sup>d</sup>
D20	p.A119T	X	9,859,054	A/G	M	SB	D	P NA	
D195	p.M1166V	X	9,900,819	G/A	F	AE, SB	D	P	NA
D56	p.S1219R	X	9,905,243	A/C	M	AE	D	D	$2 \times 10^{-4}$
TJ-QS62	p.S1251C	X	9,905,337	T/A	F	EC, SB	D	D	NA
D66	p.A1331S	X	9,905,577	T/G	F	AE, SB	D	D	$2.9 \times 10^{-4}$
SY3180	p.A1331S	X	9,905,577	T/G	F	EC	D	D	$2.9 \times 10^{-4}$
SZNT6	p.A1331S	X	9,905,577	T/G	NA <sup>e</sup>	EC	D	D	$2.9 \times 10^{-4}$
T5	p.A1331S	X	9,905,577	T/G	F	AE, SB	D	D	$2.9 \times 10^{-4}$
T9	p.G1349V	X	9,905,632	T/G	F	SB	D	D	NA
D125	p.A1470T	X	9,912,777	A/G	F	EC	D	B	$8.5 \times 10^{-5}$
D117	p.R1557H	X	9,914,796	A/G	M	SB	D	D	$5 \times 10^{-4}$
D135	p.R1557H	X	9,914,796	A/G	F	EC	D	D	$5 \times 10^{-4}$
D42	p.R1557H	X	9,914,796	A/G	F	AE	D	D	$5 \times 10^{-4}$
D44	p.R1557H	X	9,914,796	A/G	F	AE	D	D	$5 \times 10^{-4}$
D86	p.R1557H	X	9,914,796	A/G	F	AE, EC	D	D	$5 \times 10^{-4}$

*SB* spina bifida, *EC* encephalocele, *AE* anencephaly<sup>a</sup>Positions are given in bp from GRCh37<sup>b</sup>SIFT predictions: *D* deleterious<sup>c</sup>PolyPhen-2 (PP2) predictions: *B* benign, *D* probably damaging, *P* possibly damaging<sup>d</sup>MAF from the Exome Aggregation Consortium (ExAC) database<sup>e</sup>Not available